Climatic Variations in Hurricane Characteristics
And their Potential Effects on Waves and Surges in the Gulf of Mexico

Donald T. Resio, ERDC-CHL, Vicksburg, MS
Liz Orelup, Oceanweather, Inc, Cos Cob, CT

1. Introduction

The devastating 2004 and 2005 hurricane seasons along US coastal areas combined with the well documented overall rise in the number of hurricanes during the last decade or so (Goldberg *et al.*, 2001; Trenberth, 2006; Holland and Webster, 2006), have greatly increased the need to be able to examine the nature of possible future hurricane scenarios. Figure 1 from Holland and Webster (2006) suggests that we transitioned into a third tropical cyclone regime in the Atlantic basin during the mid-1990's, following a similar transition that occurred in the 1920's. Many past and ongoing studies (for example: Shapiro, 1982; Gray, 1984; Gray and Landsea, 1992; Landsea and Gray, 1992; Lighthill *et al.*, 1994; Goldberg *et al.*, 2001) have postulated causal mechanisms for these shifts in hurricane characteristics; however, few if any of these studies have examined the potential ramifications of these changes on waves and surges along specific coastlines. The purpose of this study is to examine climatic variations in large-scale atmospheric and oceanic conditions and to relate these variations to potential changes in waves and coastal surges within the Gulf of Mexico.

2. Data and Methodology

Three fundamental data sets are used in this study: 1) sea-level pressures (SLP's) from the NOATL-tropic data set (a sub-domain of the total NCEP SLP data set that covers from 0° to 40° N latitude and from 5° to 110° W longitude); 2) sea surface temperature (SST) data downloaded from Extended Reconstructed Sea Surface Temperature (ERSST); and 3) information on hurricane characteristics taken from Oceanweather, Inc files, now available in the public domain. Details on the data sets are available on appropriate web sites.

Empirical Orthogonal Functions (EOF's) have long been recognized as a powerful tool for encapsulating natural patterns within the atmosphere. In this study we used data from the 1950-2005 period (56 years) and defined 5 day mean sea level pressure (SLP) fields on a 2.5^o by 2.5^o grid. This resulted in 73 5-day intervals for every year without a leap year. Leap year was handled by adding that day into the time interval starting on February 25th, which created one element encompassing 6 days once in every 4 years. Given that we were not interested in the seasonality of hurricane but rather with the inter-annual and longer variability, we defined mean pressure fields for each 5-day interval throughout the year, with the average taken over the 56 years included in this analysis. These mean pressure fields for each 5-day interval were subtracted from the

individual mean 5-day pressure fields to produce a set of 73 x 56 pressure fields that were input into the EOF analysis.

The SST data used here represent a subset of the total ERSST data set and covers from 18° to 30° N latitude and from 58° to 98° W longitude on a 2° by 2° grid, with a land mask that restricts the data to only water points. Although SST patterns within the Gulf exhibit considerable spatial variability, it is not clear that the variations in the spatial characteristics of these patterns play a major role in the inter-annual variability of hurricane genesis and/or development. Consequently such variations are not considered here. Instead, mean monthly data for the entire Gulf of Mexico region for July through October were averaged together to provide a single measure of sea surface temperature for the each hurricane season from 1950 through 2005.

As shown in Appendix A, the data set for hurricane characteristics includes estimates of 6-hourly storm position, along with several parameters that relate to hurricane shape, size and intensity. Unlike previous data sets which have focused on short-duration (typically 1-minute maximum) wind speeds from flight level, this new data set also contains estimates of the highest sustained (30-minute average) surface-level (10-meter) wind speeds along the path of the storms. Since these are the appropriate winds for driving ocean response models, they provide a much more direct measure of hurricane surge and wave production. In some cases these wind estimates were derived primarily from simulated wind fields based on a "slab model" of the lowest region of the atmosphere combined with a planetary boundary layer model (Thompson and Cardone, 1996). In other cases these winds have been extensively reworked by analysts to assimilate available measurements.

Most past studies of climatic variability have used storm frequency (sometimes stratified by Saffir-Simpson scale) to categorize storm activity in each year. However, for our purposes we will define a single measure that incorporates both intensity and frequency into a single measure of hurricane activity. This measure of annual hurricane activity is obtained by calculating the estimated maximum kinetic energy for each storm passing through the Gulf of Mexico and adding all maxima within a given year. For any fixed time, the total kinetic energy in a hurricane can be related to storm size and storm intensity as

$$E_k \sim \iint V^2(x,y)dxdy = \iint V^2(r,\theta)rd\theta dr$$

given that $V(r,\theta) = V_{max}\phi_1\left(\dfrac{r}{R_{max}}\right)\phi_2(\theta - \theta_0)$ then

$$E_k \sim V_{max}^2 R_{max}^2$$

where V_{max} is the maximum (30-minute average, 10-m) wind speed within the storm and R_{max} is the radius to maximum winds at the same time. The value of the parameter E_k at the time of maximum wind speed during a storm's passage through the Gulf of Mexico provides a good integrated measure of the storm intensity and size at the time of the

storm's maximum intensity. Summing all values of E_k for a season yields a surrogate for combined number, size, and intensity of storms in a year.

3. Results

The EOF analysis yielded the eigenfunctions shown in Figures 2a-o. Table 1 gives the percentage of the total variance represented by each of these pressure patterns.

Table 1. Percentage of Total Variance Associated with each Eigenfunction

Eigenfunction #	Percentage Variance	Cumulative Variance
1	37.52	37.52
2	14.62	52.13
3	10.21	62.34
4	8.74	71.08
5	6.62	77.70
6	4.66	82.36
7	2.93	85.29
8	2.39	87.68
9	1.90	89.58
10	1.60	91.18
11	1.17	92.35
12	1.04	93.39
13	0.92	94.31
14	0.65	04.96
15	0.53	95.49

As can be seen in this Table, the first five eigenfunctions explain almost 80% of the total variance. Weightings on eigenfunctions for a specific 5-day interval can be defined in terms of inner products between the eigenfunctions and pressure anomaly function defined for that day, i.e.

$$1. \qquad W_{ij} = \sum_{k=1}^{N} \varepsilon_{ik}\, \hat{p}_{jk}$$

where W_{ij} is the weighting of the jth time increment on the ith eigenfunction, ε_{ik} is the value of the ith eigenfunction at the kth point in the grid, and $\hat{p}_{jk}$ is the pressure anomaly function defined for the jth time increment at the kth point in the grid. Since this analysis is focused on inter-annual variability, we first averaged the 5-day pressure anomalies to obtain a single mean anomaly field for each hurricane season. These averaged seasonal anomalies were used in defining the annual weightings on the first 15 eigenfunctions as shown in equation 1. Year-to-year variations in these weightings still contained

substantial contributions from intra-annual sources; consequently, to reduce the jaggedness of this variation through time, a running 5-year averaged value was finally derived as the best estimate of the inter-annual variability of these weightings. Figures 3-4 show variations in the weightings on the first 15 eigenfunctions through time.

As can be seen in Figures 3-4, almost all of the weightings on the eigenfunctions exhibit considerable multi-year coherency, with some of the intervals between primary maximum/minimum values covering almost the entire record length. This suggests that the atmospheric circulation in this portion of the (primarily tropical and subtropical) Atlantic is affected by factors which slowly evolve on a multi-year/multi-decadal scale. Weightings on the first four eigenfunctions do not appear to contain pronounced secular variations over this 56 year interval, although it is arguable that some systematic variation is exhibited in these time series. For example, several of the higher order eigenfunctions (notably 5, 8, 9, and 13) do appear to contain pronounced long-tern trends.

On the marine side of the boundary layer, inter-annual SST variations within the Gulf of Mexico have been shown to provide a relatively robust measure of hurricane activity within the Atlantic Basin (Holland and Webster, 2006). In fact, analyses by Holland and Webster (2006) suggest that Gulf of Mexico SST variations explain over 64% of the variations in the occurrence of major hurricanes within the entire Atlantic Basin. Figure 5 shows the variation in the average "hurricane-season" SST for the Gulf of Mexico region defined here. SST variations through time, similar to the eigenfunction weightings, exhibit substantial variability through time on a multi-year, multi-decadal time scale.

Figure 6 shows the cumulative hurricane kinetic energy per season as defined previously in this paper, smoothed over a running 5-year period. Since we are trying to extend the data as long as possible, the "smoothed" data at either end of this record is defined only in terms of the existing data within the 5-year window. For example, the 2005 data considers only data from 2003, 2004, and 2005 in its average. Thus as the ends are approached, a slight bias is created in terms of the mean position of the years contributing to this mean, culminating in a 1-year displacement at the beginning and end of the analysis along with a reduced averaging window. This Figure shows two very notable peaks, one that commenced in the late-1950's and persisted until about 1970 and a second that began around 2000 and has persisted through 2005, with a broad trough in Gulf hurricane activity between these two peaks. As with the lower order eigenfunction weightings shown in Figures 3-4, there does not appear any strong secular signal within this record. The first of these periods coincides with the very active hurricane seasons that included Hurricanes Betsy and Camille that devastated much of the central Gulf coast in 1965 and 1969, respectively, while the second contains the recent set of intense hurricanes, including Lili, Charley, Ivan, Dennis, Katrina, and Rita.

Further examination of the SST and eigenfunction weightings suggested that some very interesting relationships exist among these different measures of large-scale variability. In order to show these variations on the same scale, we first normalized all of the functions via the scaling

$$2. \qquad x_i' = \frac{2(x_i - \overline{x})}{(x_{max} - x_{min})}$$

where x_i' is the ith value of the re-scaled variate, x is the ith value of the original variate, $\overline{x}$ is the mean value of the ith variate, x_{max} is the maximum value of x for all i, and x_{min} is the minimum value of x for all i. This normalization provides a scale that goes from around -1 to around +1 for all variables and allows for improved direct visual comparisons.

Figure 7 shows a plot of SST variations and weightings on eigenfunction 1, both scaled according to equation 2 above. The consistency in the behavior of these two independently derived functions, one from purely oceanic data and the other from purely atmospheric data, is truly remarkable. The correlation coefficient between simultaneous values of SST and the weightings on eigenfunction 1 is 0.75, with a Student's T score that is significant beyond the 0.001 level. However, perusal of the two time series shows that the weightings on eigenfunction 1 appear to lead the SST variations by 1 to 2 years. Table 2 gives correlation coefficients as a function of the phase difference between the SST pattern and the weightings on eigenfunction 1. As can be seen here, the time-shifted correlation function seems to attain its maximum value when the SST pattern is lagged behind the EOF pattern by 1 to 2 years. This is extremely intriguing since it suggests that trends in weightings on eigenfunction 1 can be used to predict future trends in SST within the Gulf of Mexico. As can be seen in this Figure, given that the relationship between weightings on eigenfunction 1 and SST persist into the future, the near-term trend in the average Gulf-wide SST is predicted to be downward. So far, this year's values (2006) appear to agree with this trend, since the temperatures are, in fact, running slightly less than last year's.

Table 2. Correlation coefficient between weightings on EOF 1 and SST as A function of time difference between the two series.

LAG (years)	Correlation Coefficient	Student's T
-3	0.72	7.426
-2	0.79	9.251
-1	0.79	9.243
0	0.75	8.342
1	0.61	5.571
2	0.48	3.908
3	0.39	3.032

Another interesting relationship can be seen when we add scaled weightings on eigenfunction 3 to the plot of SST and EOF weighting variations through time. Figure 8 shows that weightings on eigenfunction 3 appear to be lagged even more behind variations in weightings on eigenfunction 1 than the SST patterns. Since each individual eigenfunction is constrained to be orthogonal to all of the other eigenfunctions, it is typically assumed that these eigenfunctions are unrelated. Figure 8 shows that the lack of correlation in this case is due to a phase shift, much in the manner of the orthogonality that exists between sine and cosine functions. However, from a perspective of predictability, it can be seen that the weightings on eigenfunction 3 can be estimated relatively well from preceding weightings on eigenfunction 1 and SST within the Gulf of Mexico. As was the case with the relationship between SST's and weightings on eigenfunction 1, the time-shifted correlation between SST's and weightings on eigenfunction 3 attain maximum values of approximately 0.79 in the 1 to 2 year displacement range; but in this case, SST variations lead the eigenfunction 3 weighting variations. For completeness, we computed the time-shifted correlations between weightings on eigenfunction 1 and on eigenfunction 3. A maximum value of 0.66 was attained for eigenfunction 1 leading eigenfunction 2 by about 3 to 4 years.

Figure 9 shows a schematic representation of SST variation through time, in terms of a single 40-year harmonic, along with the variation in cumulative kinetic energy per season. This figure suggests that the Gulf SST pattern might lead Gulf hurricane activity by about 5-6 years, at least in terms of the time between the peaks. From many of the papers published on this topic, we might expect closer synchronization between SST variations and hurricane activity; however, it is likely that a number of other factors/cycles within the global ocean-atmospheric system are also contributing to this pattern in the Gulf of Mexico in addition to the SST's. In particular, SST variations in Atlantic regions outside of the Gulf of Mexico have been shown to contain a very significant secular trend; and many of the higher order eigenfunctions exhibit varying phase shifts from the SST pattern, which suggests that the sum of many more effects might have to be considered to predict hurricane activity.

Based on the pattern of variation seen in the eigenfunction weightings and SST's, shown in Figure 9, the current episode of hurricane activity might be considered as an analogue to about the first half of the 1960-1970 epoch of intense hurricane activity within the Gulf of Mexico. It should be noted that not every year in the 1960-1970 period contained a major hurricane within the Gulf, so it appears possible that, even during intervals of high hurricane activity, some years can be fairly quiescent. If this analogue holds true, however, we should expect about 5 more years with relatively high hurricane activity in the Gulf.

4. The effect of climatic variations on extremes

One of the basic tenets in extremal estimation is that estimates of return periods should be based on samples drawn from homogeneous populations. Since hurricane

activity appears to depend quite strongly on eigenfunction weightings and SST's, it makes sense to stratify the record on the basis of the phasing shown in Figure 9. In this context, the expected long-term probability of a given event can be defined as

$$3. \qquad P(x) = \int P(x \mid \vec{S}) p(\vec{S}) d\vec{S}$$

Where, $P(x)$ is the expected long-term probability of x, and $\vec{S}$ is the vector of large-scale atmospheric and oceanic factors that pre-condition these probabilities in a particular year. Since we have only a limited data set, it is difficult to stratify our sample into a large number of categories and still retain a useful sample size; consequently, we shall use the primary phase of the cycle shown in Figure 9 as the single stratification criterion to be investigated here. For simplicity and to retain as much sample size as possible within each category, we shall consider only 2 categories: Group 1 – which covers phase angles from 0° through 89° and 181° through 359° (low activity years); and Group 2 – which includes phase angle 90° through 180° (high activity years).

Table 3. Landfalling central pressures for Group 1 and Group 2

Group 1 (39 years)			Group 2 (17 years)		
Year	Name	Central pressure (at landfall)	Year	Name	Central pressure (at landfall)
1957	Audrey	963.6	1961	Carla	936.4
1974	Carmen	942.8	1964	Hilda	960.0
1979	Frederic	949.7	1965	Betsy	945.2
1980	Allen	945.0	1967	Beulah	950.0
1992	Andrew	949.0	1969	Camille	905.8
1996	Opal	940.2	1970	Celia	944.0
1999	Earl	953.0	2002	Lili	966.3
			2004	Charley	950.2
			2004	Ivan	955.1
			2005	Dennis	951.9
			2005	Katrina	919.4
			2005	Rita	945.8
			2005	Wilma	951.1

As can be seen from this Table 3, the frequency of storms in Group 1 is only 0.137 storms per year; whereas the frequency of storms in Group 2 is 0.765 storms per year, which is about 5.5 times higher. Combining these storms into an appropriate form for estimating return periods, T(x), yields

$$T(x) = \frac{1}{1 - \sum_n \lambda_n \beta_n F_n(x)}$$

where

4. λ_n is the frequency of storms in Group n

      $F_n(x)$ is the cumulative distribution function (CDF) for storms in Group n

      and β_n is the proportion of years in Group n

In many applications, the populations can occur in the same year (for example the largest extratropical event per year and the largest tropical event per year). In this case, $\beta_n \equiv 1$ for all n. An interesting attribute of the equation written in this form is the if all of the CDF's were the same, it could be simplified into the form

5.
$$T(x) = \frac{1}{1 - F(x) \sum_n \lambda_n \beta_n}$$

      where F(x) is the general CDF for all Groups.

however, it must first be shown that all of the CDF's are equivalent.

The GEV solution for an asymptotic distribution of x can be written as (Jenkinson, 1955)

$$F(\hat{x}) = e^{-e^{-\hat{x}}}$$

6.   where

$$\hat{x} = A + B\left(\frac{1 - e^{-Cx}}{C}\right)$$

where A, B, and C are three parameters of the GEV distribution. In the case where $C \to 0$, this distribution becomes the Fisher-Tippett Type I, or Gumbel, distribution, which can be written as a function of only 2 parameters, i.e.

$$\hat{x} = \frac{x - a}{b}$$

where a and b are the Gumbel distribution parameters. Since we have a relatively small sample size, we shall use the 2-parameter Gumbel form of this equation, rather than the complete 3-parameter form. Figure 10 shows the results for the Gumbel analysis of Group 1, Group 2, all storms considered as one population, and populations combined via equation 4. As can be seen here, equation 4 behaves like the combined-population analysis up to the point where the Group 2 storms begin to dominate, at which point it

begins to follow that distribution; thus, it is a better method for extrapolations than treating the two separate populations in a combined analysis. Two important points can be argued from information shown in Figure 10. First, a sample from a climatic regime (low-activity years) that does not contain a representative proportion of the climatic regime with controls the extremes does not provide a realistic estimate of the expected extremes. Second, in situations in which threat levels vary markedly from one large-scale regime to another, they should not be combined into a single analysis for estimating extremes. In the case shown here, the treatment of hurricane threat as though the two separate levels of hurricane threats could be represented as a single populations leads to an underprediction of the expected central pressure by about 5 mb at the 100-year return period.

Assuming stationarity in all the factors which influence these variations in hurricane activity, Figure 10 should provide a reasonable assessment of the hurricane threat along the Gulf of Mexico, at least in terms of storm intensity (as indicated by central pressure at landfall). However, as noted several times in this paper, work by many others has shown a significant secular trend in SST values over the rest of the tropical and subtropical Atlantic basin. Because of this and the fact that many of the eigenfunctions do appear to contain secular trends in their weightings through time, it is likely that there will be some level of secular variation expected within the Gulf of Mexico during the next century. Given the potential impact of such variation on coasts and the people inhabiting coastal areas, it is critically important to examine future scenarios in as objective a manner as possible. Table 4 presents correlations between first 15 eigenfunctions in this study and the annual cumulative kinetic energy, defined as described above.

Table 4. Correlations Between Annual Cumulative Kinetic Energy and Eigenfunction Weightings

(Underlined Student's T Scores Designate Significance above the .99 Level of Confidence)

Eigenfunction	Correlation	Student's T
1	0.1493216	1.109727
2	-0.2459255	1.864435
3	-0.3340233	2.604129
4	-0.1314833	0.9746628
5	-0.1915766	1.434362
6	-7.9412408E-02	0.5854084
7	-0.1434847	1.065417
8	-0.2273055	1.715246
9	1.8339736E-03	1.3476920E-02
10	-5.3688638E-02	0.3950992
11	0.2781583	2.128020
12	0.3209944	2.490618
13	-0.4129986	3.332384
14	0.4549139	3.753832
15	0.2868412	2.200305

As can be seen in this Table, many of the eigenfunctions, particularly some of the higher order eigenfunctions, are significantly correlated with annual cumulative kinetic energy. Weightings on many of these higher order eigenfunctions, when scrutinized in Figure 4, contain trends as well as cycles within them. Thus, the next five years will probably not be an exact analogue to the late 1960's. In particular, weightings on eigenfunctions 11, 13, 14, and 15, all of which appear to be correlated with hurricane activity, all exhibit opposite signs during the recent 5 years from their weightings during the 1960's.

It is also interesting to note that, whereas SST's in the Gulf of Mexico have not shown a significant trend over the last 56 years, SST's in the rest of the Atlantic basin have. Figure 11 shows the variation in the average SST for the Atlantic basin between the equator and 30° N latitude, with land areas and the region already considered within the Gulf of Mexico removed. As has been shown in many papers and apparent in Figure 11, SST's have been climbing fairly steadily since the mid 1970's. Thus, there is certainly ample reason to speculate on what effect possible future climate scenarios would have on the hurricane threat in the Gulf of Mexico.

If we assume that the percentage of time in atmospheric and oceanic states that are equivalent to Group 2 were to double over the next 40 years, the consequence would be essentially a doubling of the frequency of storms with central pressures less than about 930 mb. Such a situation would be consistent with the indications of Holland and Webster (2006) shown in Figure 1. As shown in Figure 12 based on a doubling of the relative frequency of high-activity years in equation 4, this would shift the central pressure at any fixed return interval above 5 years by about 10 mb. This is around the twice the magnitude of shift caused by treating the 2 Groups of hurricanes separately via equation 4, rather than combining the populations into a single GEV analysis.

5. Extension to the impacts of climatic variability on waves and surges within the Gulf of Mexico

In order to ascertain the impact of variations in hurricane frequency-intensity on surges and waves within the Gulf of Mexico, it is necessary to postulate quantitative relationships between central pressures and surges and between central pressures and waves in hurricanes. Following the work of Resio and Perrie (1989) and Resio *et al.* (2004), waves within a hurricane are expected to scale as

$$\hat{H}_{max} \sim \hat{t}^{5/7}$$

where

7. $\hat{H}_{max} = \dfrac{gH_{max}}{u^2}$ is nondimensional wave height

and

$\hat{t} = \dfrac{ut}{g}$ is nondimensional time

In equation 7, H_{max} is the maximum significant wave height in a storm, g is gravity, u is a typical wind scaling parameter (for example the average over some fixed time at a 10-meter level), and t is time. Similar to the argument made in deriving the proportionality for the total kinetic energy in a storm, one can show that the maximum significant wave height in a hurricane can be written in terms of proportionality involving standard hurricane parameters,

$$8 \qquad H_{max} \sim \frac{u_{max}^{9/7}}{g^{2/7}} \left(\frac{R_{max}}{V_f'} \right)^{5/7}$$

where V_f' is the effective forward velocity of the hurricane, given by

$$9. \qquad V_f' \sim \frac{R_{max}}{(<V_f - c_g>)}$$

where V_f is the actual forward speed of the hurricane, c_g is the group velocity of the waves, and the brackets $<>$ denote an averaging of the nonlinear interaction between the moving storm and propagation effects within the wave field. Hence,

$$H_{max} \sim \frac{u_{max}^{9/7}}{g^{2/7}} \left(<V_f - c_g> \right)^{5/7}$$

Analysis of the forward velocities in hurricanes shows no significant variations between Group 1 and Group 2 storms. Similarly, the relationship between R_{max} and Δp seems quite consistent between the two groups. This suggests that expected variations in the maximum significant wave heights should be related primarily to expected variations in wind speed. Figure 12 shows the derived relationship between maximum wind speed in a storm and Δp, based on Vickery's HBL model (Vickery *et al.*, 2000), with Oceanweather's estimated maximum (30-minute) maximum wind speed for all storms in the Gulf of Mexico. Over the range shown here, this relationship is reasonably linear.

Since R_{max} is included in the argument for the variation in maximum significant wave height, it must be considered in the final integral for the expected variation in maximum wave height,

Irish *et al.* (2007) has shown that, on an idealized coast with a constant sloping bottom and a wall at the coast (perhaps similar to the situation of a hurricane protection levee in some areas of the Gulf), with the coefficient of drag capped as found in recent studies, the relationship between surge height at the coast and wind speed can be approximated as

$$\eta_{max} \sim \frac{u_{max}^2}{g} \Psi(\hat{R}_{max})$$

10.   where R_{max} is a nondimensional storm size parameter, given by

$$R_{max} = \frac{gR_{max}}{u_{max}^2}$$

In this case, it is important to recognize that storm surge is also quite dependent on storm size, as well as wind speed. It should be noted at this point that more intense storms tend to be smaller than weaker storms. Whereas, storm size could be factored out of the expected wave height variation, it cannot be factored out of equation 10. Using relationships from Irish *et al.* (2007) coupled with the expected covariation of storm size and pressure differential, we can obtain the estimate of the expected impact of a doubling in the number of active hurricane years (Group 2 years).

Table 5 gives the estimated variation in maximum significant wave heights and coastal storm surges for the central Gulf region, given a doubling in the frequency of active hurricane seasons.

Table 5. Estimated changes in extreme waves heights and surges for selected return periods, given a doubling of years with high hurricane activity.

Return Period (years)	Change in Wave Height (percent)	Change in surge (percent)
25	+15	+18
50	+13	+16
100	+12	+15
250	+11	+12
500	+10	+ 9

Estimates such as shown in Table 5 should not be taken as an absolute estimate of what will happen as we move into the future, but certainly provide valuable information on the

potential magnitude of changes in the hurricane threat along the central Gulf coast. This is one more factor that should be considered in the assessing long-term risks due to hurricanes in this area, along with expected long-term subsidence and likely changes in the coastal landscape.

6. Discussion and conclusions

This paper has addressed several aspects of hurricanes and their affects on waves and surges within the Gulf of Mexico. Key points are summarized below.

Variations in SLP and SST's within the Gulf of Mexico:

An EOF decomposition of SLP patterns within a selected tropical/subtropical region of the northern hemisphere has shown a very close relationship between variations in SLP patterns and average hurricane-season SST's within the Gulf of Mexico. Unlike the remainder of the Atlantic basin, Gulf SST's do not exhibit a strong secular trend, but rather exhibit a roughly cyclical variation with peaks around 1960 and the early 2000's. A very interesting finding is the apparent 1-2 year phase lead between weightings on the first eigenfunction and SST's within the Gulf. If this link persists, it is expected that SST's within the Gulf will diminish during the next few years, following its peak during 2005.

The effect of climatic variability on hurricane characteristics

Hurricane frequency and intensity have both varied substantially over the 1950-2005 period; but this variability does not seem to be associated with a clear secular increase in activity over this period of record. Instead, highest levels of hurricane activity appear to be associated with the falling phase of cycles in weightings on the first eigenfunction and SST's in both the 1960's and early 2000's. If the rough analogue between the 1960's and the 2000's persists, the central Gulf coast can expect about 5 more "high activity" years in this cycle, followed by a return to a less active period. It is important to note here that individual years within a "high-activity" epoch can be relatively quiescent, such as 1962, 1963, and 1968 during the 1960's period of high activity. Thus, the relatively calm 2006 season up to through mid September of this year should not be interpreted as indicating that the high-activity period is over.

Extremal estimation of central pressures given strong decadal and multi-decadal variations in hurricane characteristics

The distribution of central pressures in hurricanes during "high activity" years varies substantially from its distribution during "low activity" years. For example, the estimated 100-year central pressure based on only "low activity" years is 933 mb, while the 100-year central pressure for "high activity" years is 906 mb. Although larger extremes (higher pressure differentials) are dominated by "high activity" years, improved estimates of expected return periods can be obtained via the appropriate combination of

two separate populations, rather than by assuming that these two populations are equivalent.

Estimated changes in wave heights and coastal surges related to hurricane variability

Given the scaling relationships that exist in the wave generation process, it is shown here that the maximum significant wave height in a hurricane is expected to be proportional to wind speed to the 9/7 power. Additional analyses can be used to show that wind speed is approximately linearly related to pressure differential (peripheral pressure minus central pressure) over a fairly wide range of central pressures. In a scenario in which the frequency of "highly active" years were to increase by a factor of 2, estimated 100-year significant wave heights in the Gulf of Mexico would be expected to increase by about 12%. A similar analysis shows that the same doubling of "highly active" years would lead to approximately a 15% increase in coastal surge levels at the 100-year return period. The conclusions summarized should not be construed as arguing that there will be a doubling of "highly active" years in the near future, but only as providing some guidance on how much such a change would affect waves and surges in the Gulf of Mexico.

REFERENCES

Goldberg, S.B, Landsea, C.W., Mestas-Nunez, A.M. and W.M. Gray, 2001: The recent increase in Atlantic hurricane activity: Causes and implications, *Science*, 293, 474-479.

Gray, W.M., 1984: Atlantic seasonal hurricane frequency. Part II: Forecasting its variability, *Mon. Wea. Rev.*, 112, 1649-1668.

Gray, W.M. and C.W. Landsea, 1992: African rainfall as a precursor of hurricane-related destruction on the U.S. east coast, *Bull. Amer. Meteorol. Soc.*, 73, 1352-1364.

Holland, G., 1980: Analytic model of the wind and pressure profiles in hurricanes, *Mon. Wea. Rev.*, 112, 1649-1668.

Holland, G.J. and P.J. Webster, 2006: Heightened tropical cyclone activity in the North Atlantic: Natural variability or climate trend? *Proc. Roy. Soc. A,* (submitted).

Irish, J.L., Resio, D.T. and J.J. Ratcliff, submitted for publication: Hurricane surge
characterization. In preparation for Journal submission.

Jenkinson, A.F., 1955: The frequency distribution of annual maximum (or minimum)
Values of meteorological elements, Quart. J. Roy. Met. Soc., 81, 158-171.

Lighthill, J., *et al.*, 1994: Global climate change and tropical cyclones, *Bull. Amer.
Meteorol. Soc.,*, 75, 2147-2157.

Resio, D. T. and W. Perrie, 1989: Implications of an f^{-4} equilibrium range for wind-
generated waves, *J. Phys. Oceanogr.*, *19*, 193-204.

Resio, D.T., C.E. Long, C. L. Vincent, 2004: Equilibrium-range constant in wind-
generated wave spectra. *J. Geophys. Res..*, 109, C01018, doi:10.1029/2003JC001788.

Shapiro, L., 1982: Hurricane climatic fluctuations. Part II: Relation to large-scale
circulation. *Mon. Wea. Rev.*, 110, 1014-1023.

Thompson, E.F. and V.J. Cardone, 1996: Practical modeling of hurricane surface wind
fields. J. Wtrwy. Port, Coastal, and Ocean Engr., ASCE 122, 195-205.

Trenberth, K.E. and D.J. Shea, 2006: Atlantic hurricanes and natural variability in 2005,
Geophys. Res. Lett. , In press.

Vickery, P.J., Skerjl, P.F., and L.A. Twisdale, 2000: Simulation of hurricane risk in the
U.S. using empirical track model, *J.Struct. Engr.*, 1222-1237.

North Atlantic Tropical Cyclones 1905-2005
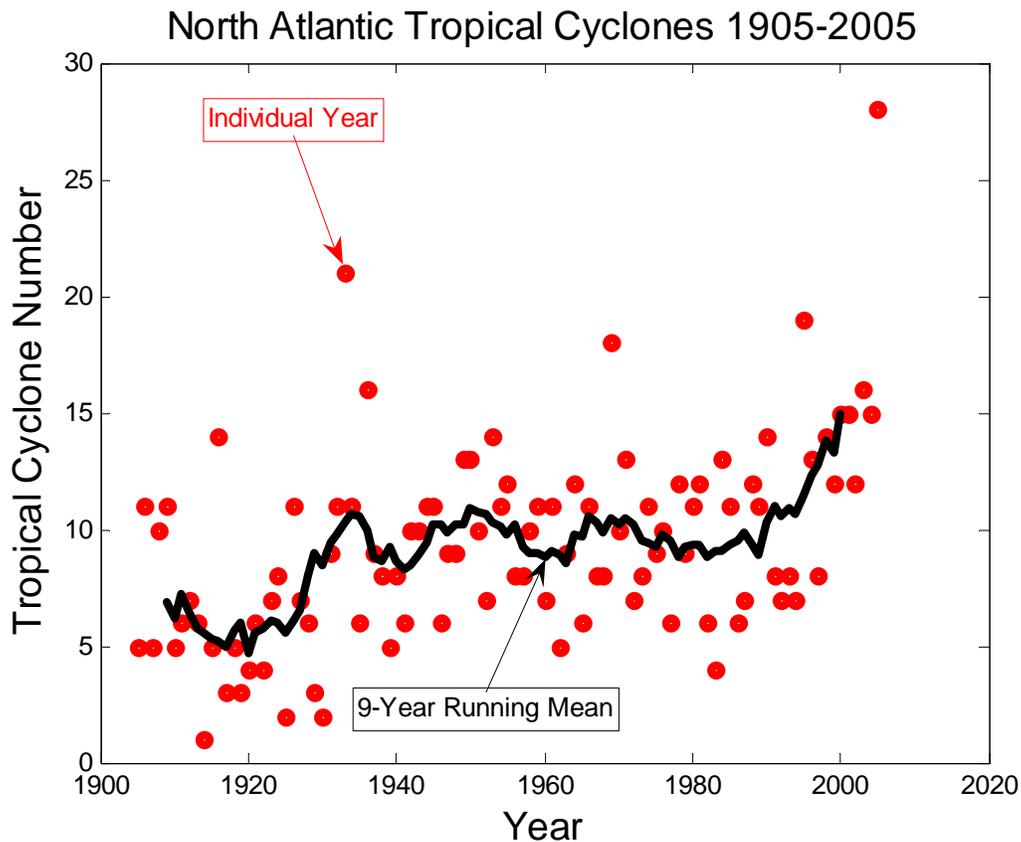
Figure 1. Plot of average number of Tropical Cyclones in the Atlantic Basin: 1900-2005, from Holland and Webster (2006). As noted in Figure, red dots designate numbers for individual years, while the black line is the 9-year running average number of storms.

5 Day Mean SLP Anom Eigen Vectors NOATL 0-40N, 110-5W: June 30-Nov 1, 1950-2005
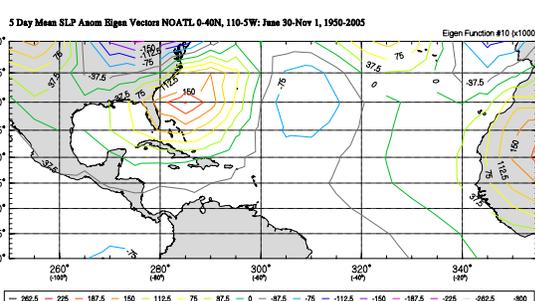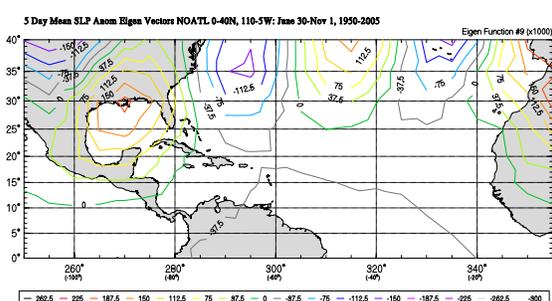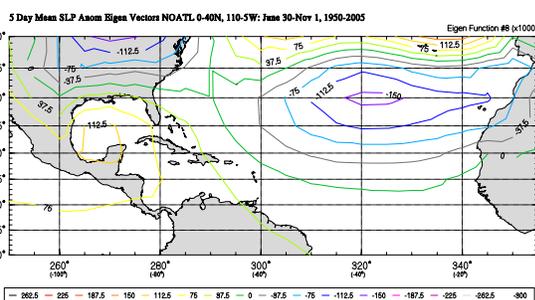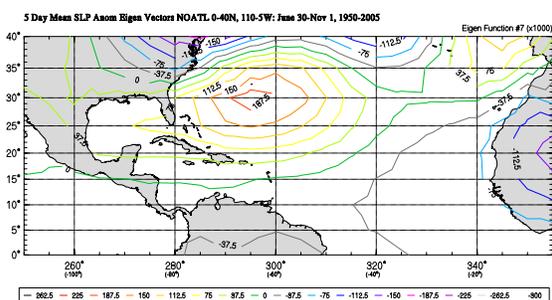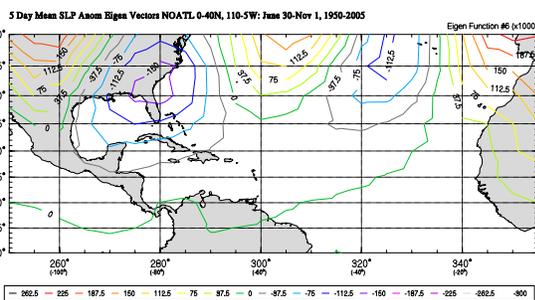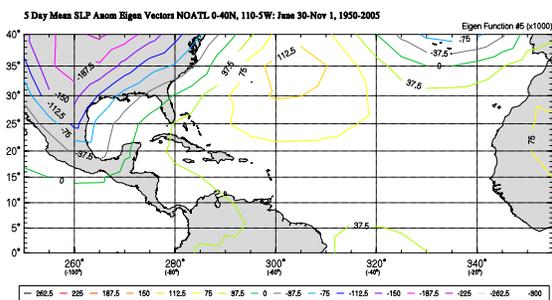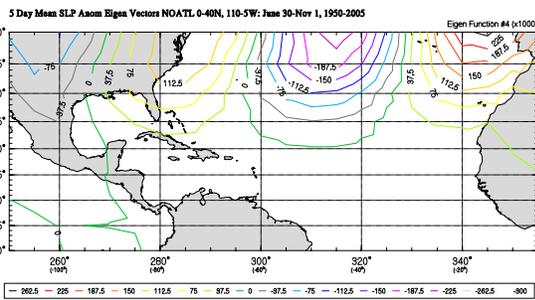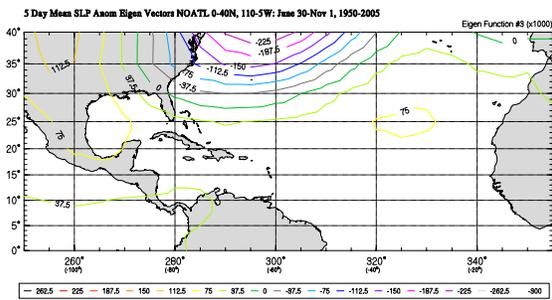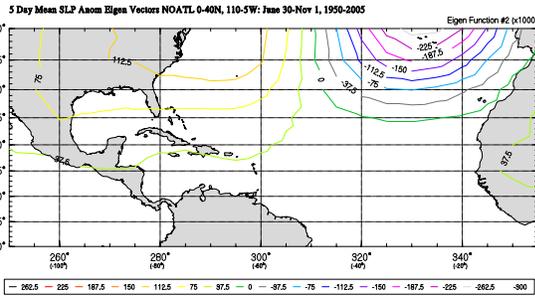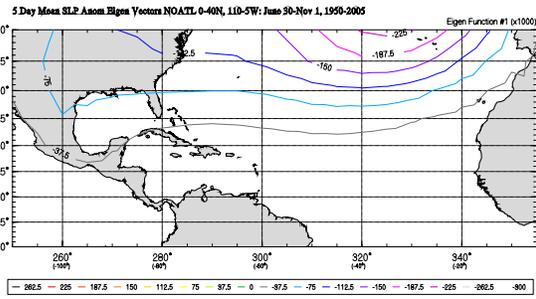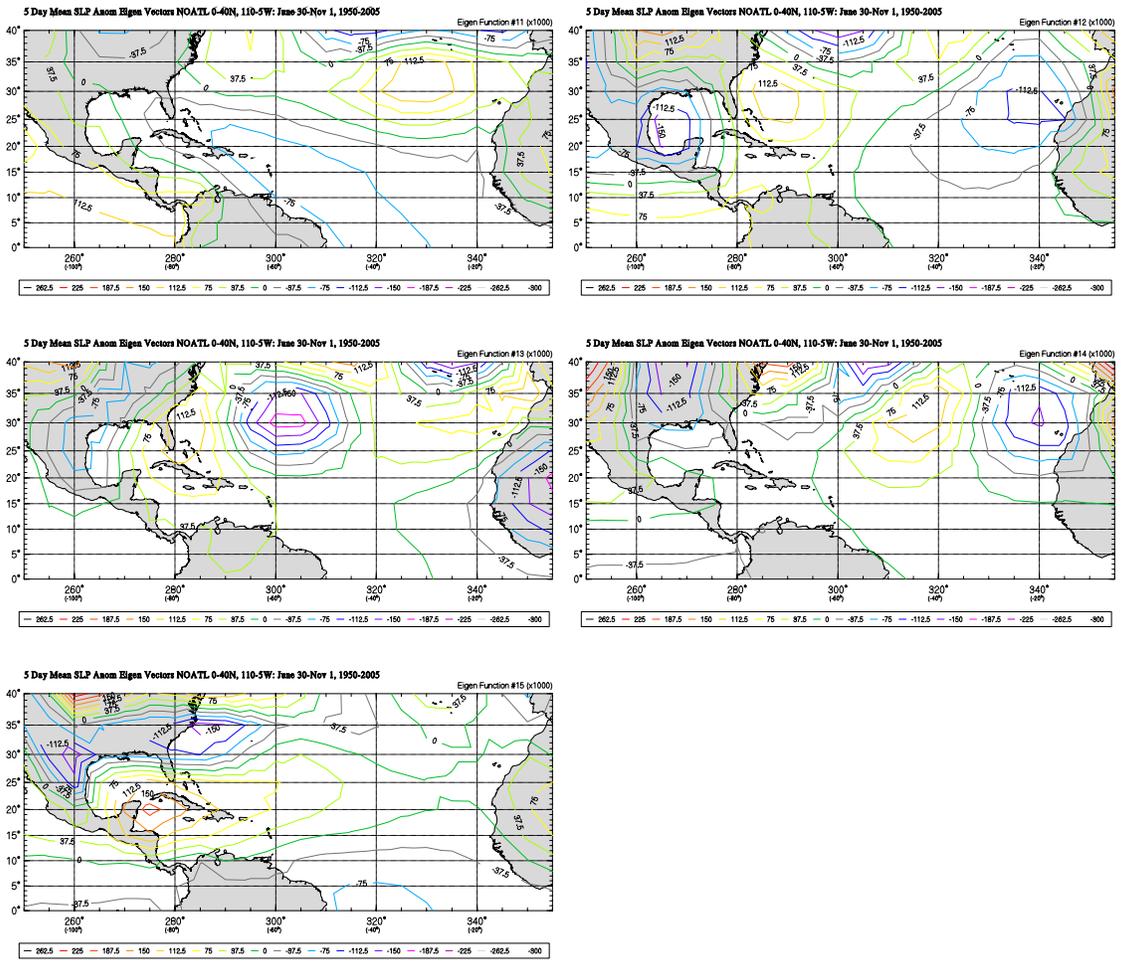
Figure 2 (a-o). Eigenfunctions 1-15.
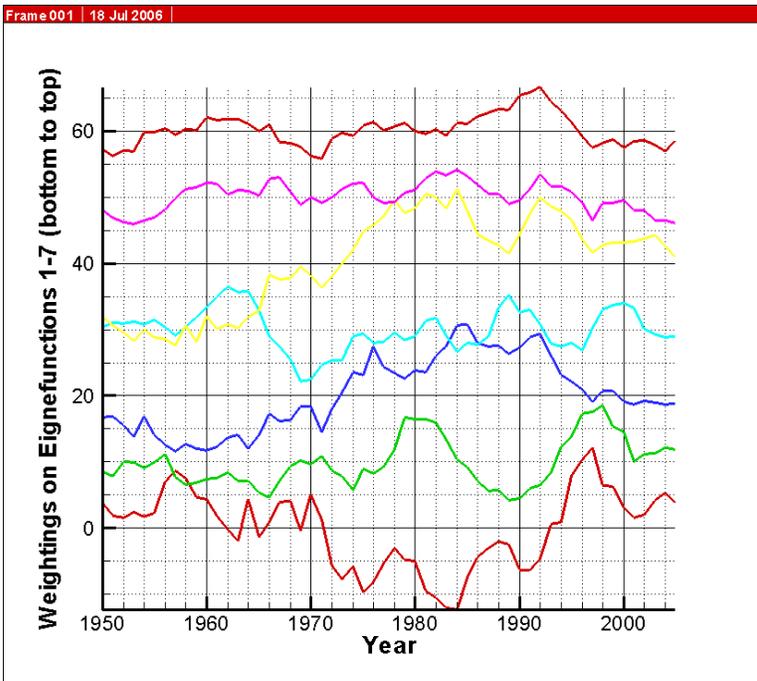
Figure 3. Weightings on eigenfunctions 1-7: 1950-2005. For clarity in this figure, a constant equal to (n-1)x20 is added to these weightings where n is the eigenfunction number.
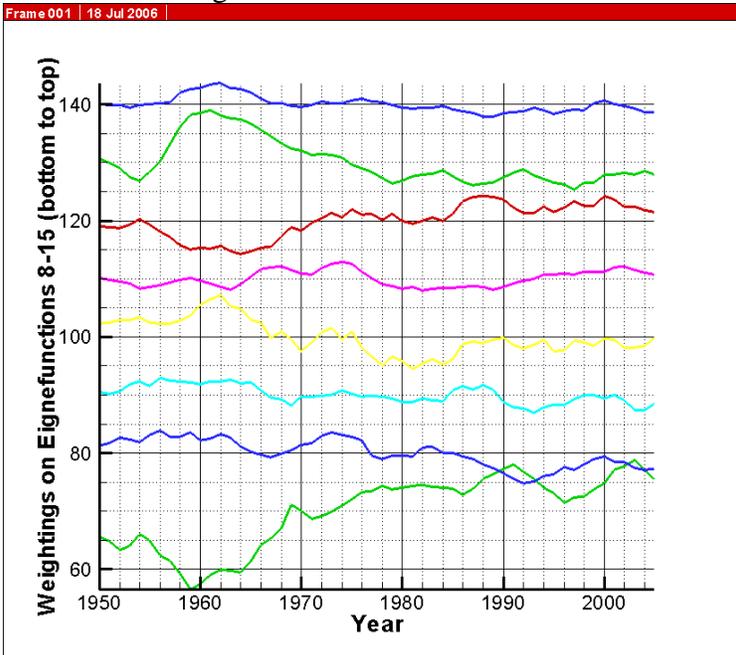
Figure 4. Weightings on eigenfunctions 8-15: 1950-2005. For clarity in this figure, a constant equal to (n-1)x20 is added to these weightings where n is the eigenfunction number.
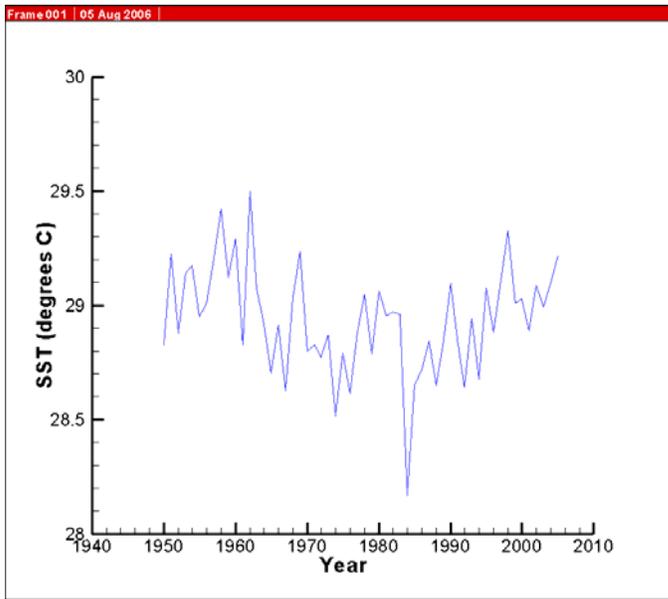
Figure 5. Plot of average SST for Gulf of Mexico: 1950-2005.
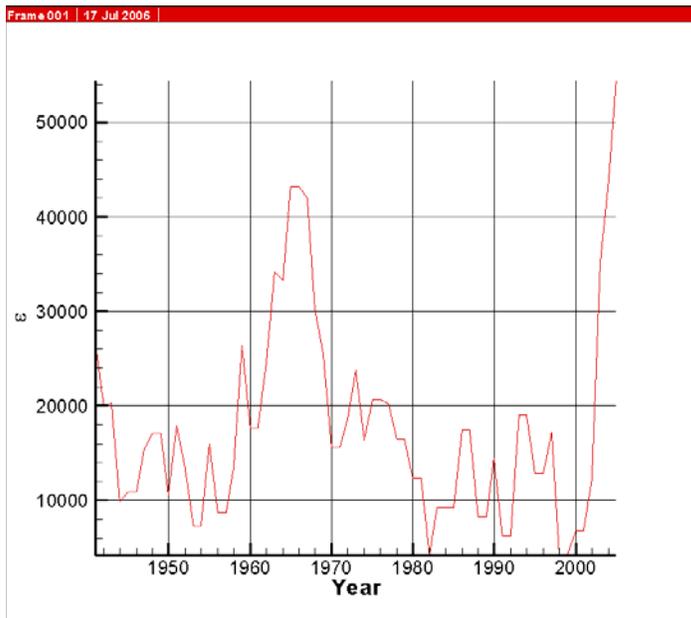
Figure 6. Plot of estimated cumulative kinetic energy for all storms at time of maximum surface winds within each year: 1940-2005.
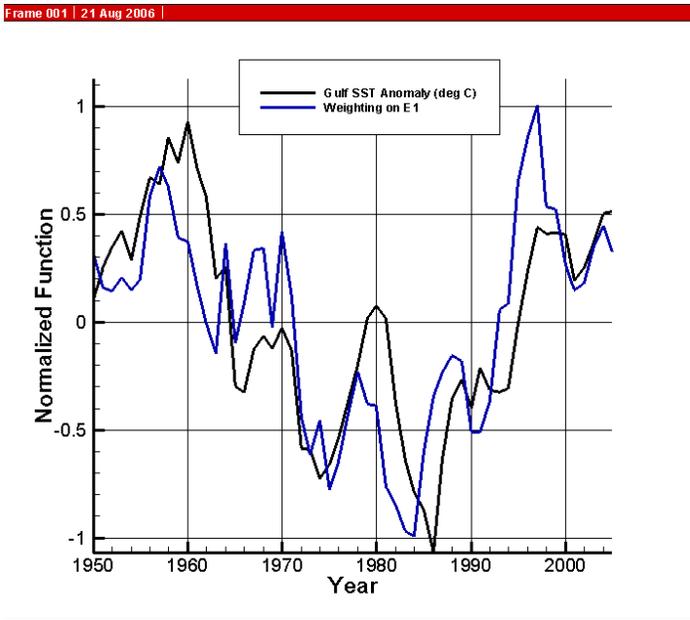
Figure 7. Plot of scaled values of SST and weightings on eigenfunction 1 through time – incorporating scaling shown in equation 2.
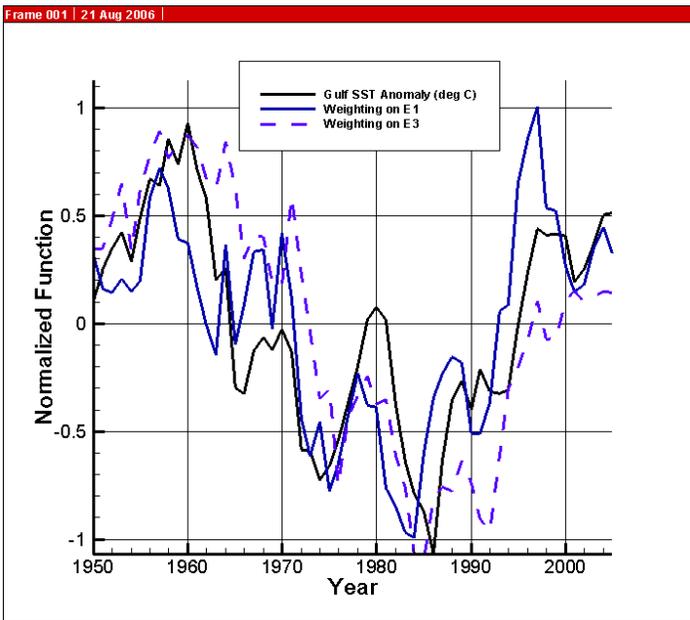
Figure 8. Same as Figure 7 but with weightings on eigenfunction 3 added.
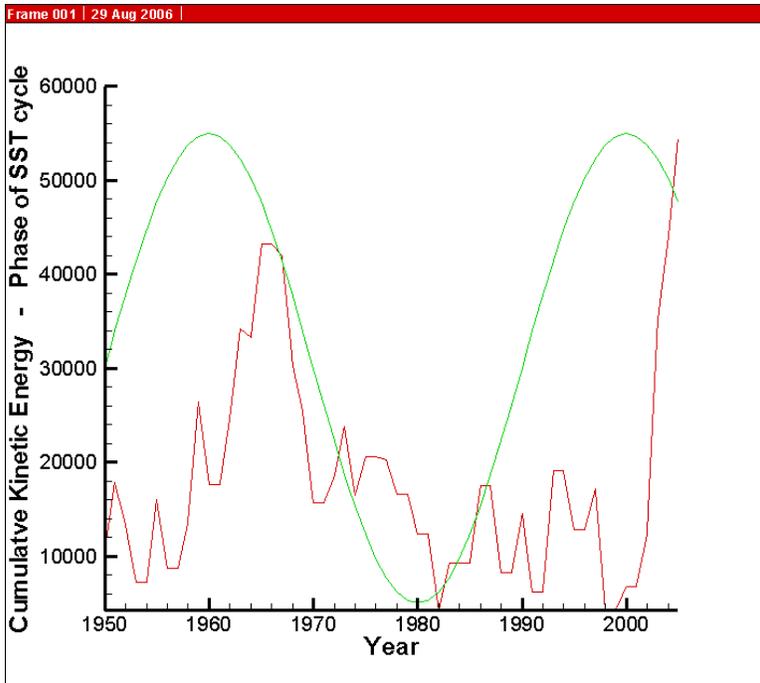
Figure 9. Variation of hurricane activity as indicated by the
cumulative kinetic energy per season from 1950 through 2005
along with the phase of the Gulf of Mexico SST cycle.
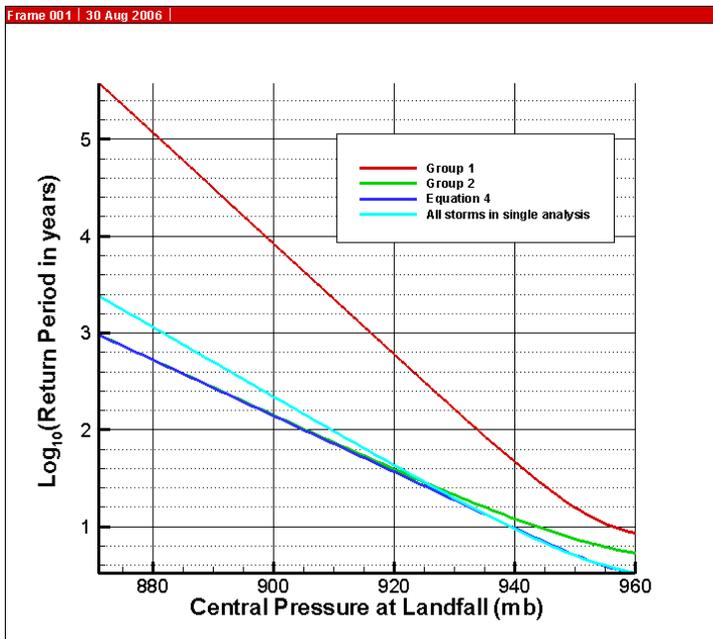
Figure 10. Estimated return periods for 4 separate analyses:
Group 1 alone; Group 2 alone; Groups 1 and 2 combined
into a single analysis; and estimate based on equation 4.
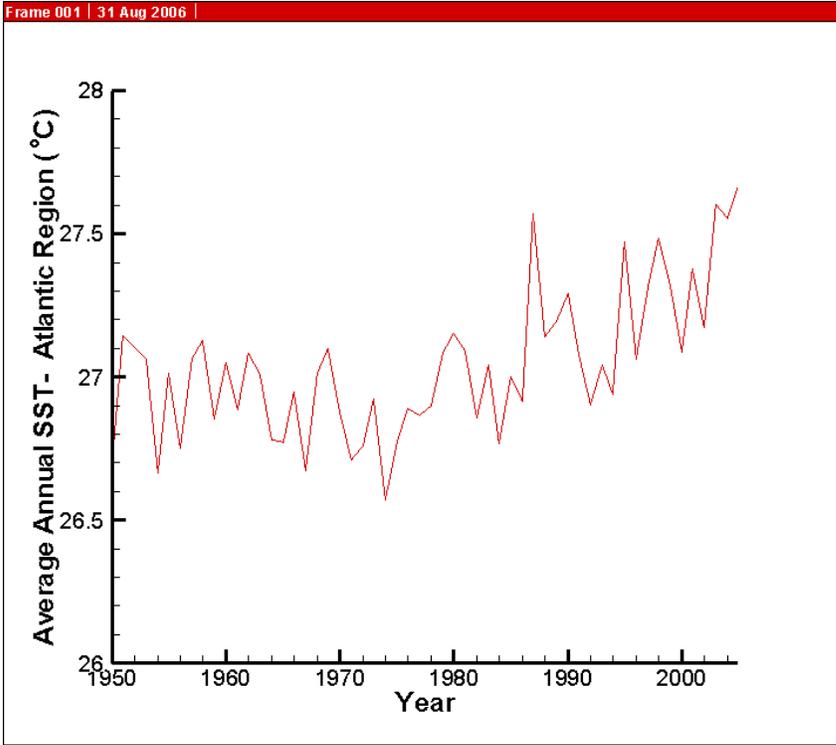
Figure 11. Average annual SST values for the North Atlantic basin between the equator and 30° N latitude with the Gulf of Mexico removed.
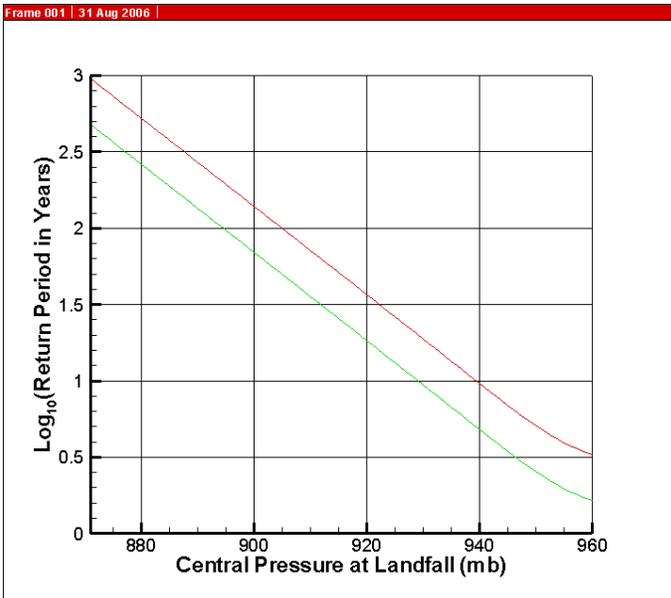
Figure 12. Effect of doubling frequency of time within Group 2 large-scale atmospheric-oceanic state. Red line denotes current conditions. Green line denotes post-doubling conditions.
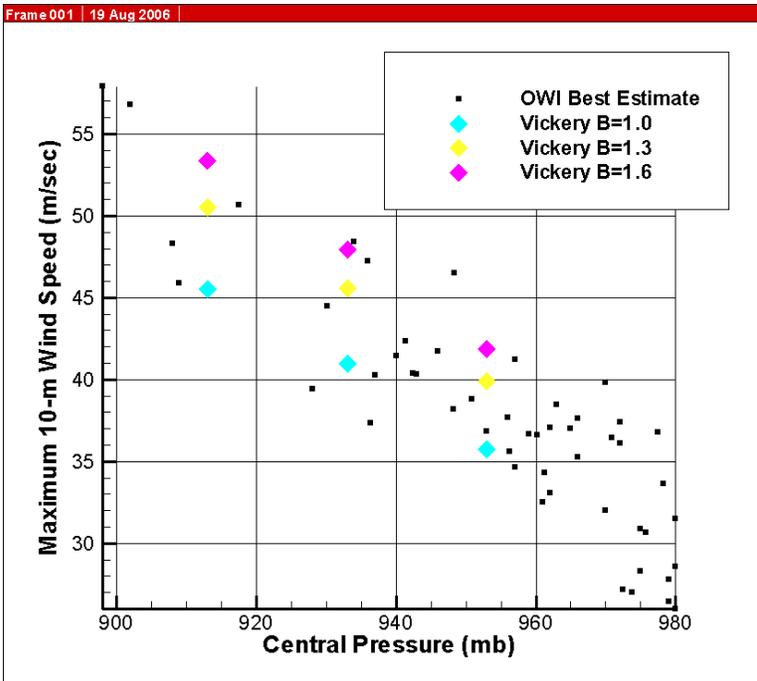
Figure 13. Comparison of Maximum wind speed in a hurricane estimated from Vickery's HBL model (Vickery, 2006), for Holland B values of 1.0, 1.3, and 1.6, given a forward speed for the storm of 5 m/sec to "best-estimate" maximum surface wind speeds in actual Gulf of Mexico storms from Oceanweather, Inc.